Non-linear kalman filters for battery state of charge estimation and control

(Article begins on next page)

02 March 2024

Non-linear Kalman Filters for Battery State of Charge Estimation and Control

Alessandro Rizzello, Santo Scavuzzo, Ettore Bianco, Massimiliana Carello
DIMEAS
Politecnico di Torino
Torino, Italy

Alessandro Ferraris,, Andrea Giancarlo Airale
BEOND SRL
Torino, Italy

Abstract—In this paper, two different non-linear Kalman Filters for lithium-ion battery state of charge estimation are presented and compared. Nowadays, lithium-ion batteries are extensively used for hybrid and electric vehicles; in such applications, cells are assembled in module and pack to achieve high performance. At this scope, a Battery Management Systems BMS is required to control each cell and improve the battery pack performance, safety, reliability, and lifecycle. One of the major tasks a BMS must fulfill is an accurate online estimation of the State Of Charge (SOC) of the battery pack. In this paper, the Extended Kalman Filter and Sigma Points Kalman filter are developed and compared. A battery equivalent circuit model has been chosen to have a good compromise between complexity and accuracy and model parameters have been identified from Hybrid Pulse Power Characterization (HPPC) tests carried out at different temperatures and current rates to obtain a model valid for a wide range of operating conditions. The SOC estimation strategies are developed starting from the experimental results and it is validated through different driving cycling simulations. The results show that the Sigma Points Kalman filter produces a better estimate of SOC with respect to the Extended Kalman Filter, due to its better capability to deal with system non-linearities, with comparable computational complexity.

Keywords—Battery, Control, Kalman filter, State of Charge, Experimental validation

I. INTRODUCTION

In the last few years, the increased awareness of the impact of fossil fuels on the environment has justified the need for a strong development of renewable energies [1]. The automotive sector is a major contributor to greenhouse gas emissions; thus, a great effort is being made for fleet electrification today. An important feature of Electric vehicles, EVs, and hybrid electric vehicles, HEVs, is the higher efficiency of the electric motors involved which present an overall efficiency of up to 96% compared to the efficiency of Internal Combustion Engine ICE of 18-20% [2] - [3]. Other advantages of electric motors are the lower number of moving components which imply low maintenance compared to ICEs, but the most important feature of electric motors is their power characteristic curve able to deliver high torque at low speed which makes a multi-speed gearbox unnecessary. Among all battery chemistries Lithium-ion cell is the most widespread technology for energy storage in hybrid and electric vehicles due to their high intrinsic safety, fast charging, small dimensions, weak memory effects, and long cycle life. On the other hand, the cost of materials and manufacturing remains not negligible.

The automotive application requires both high power and energy, thus a huge number of cells must be connected in series and in parallel to fulfill the vehicle requirements. During its operation, each cell faces a wide range of working conditions characterized by extremely dynamic current profiles and different temperatures, thus they must be controlled to verify and enhance safety and performance, this task is carried out by the battery management system, BMS. It must be able to evaluate the battery status in terms of state of charge SOC, state of health SOH, and cell aging.

The market penetration of the electric and hybrid electric vehicles is still low due to some limitations such as high battery price, poor charging infrastructure, long charging time, and range anxiety, which is justified by the very low specific energy of battery pack equal to around 0.25 kWh/kg compared to fossil fuel vehicle which is equal to around 13 kWh/kg [4].

One way to solve partially the issue of range anxiety is to evaluate accurately the residual energy inside each cell of the battery pack. Nevertheless, two main issues occur: first, it is impossible to directly measure this quantity, second, the capacity of each cell is affected by temperature, current profile, and aging conditions, thus dedicated algorithms must be developed which are able to take into account the dependency from these quantities. An accurate estimation of the SOC is required because it increases the performance, lifetime, and safety of the battery pack. The battery pack performance can be enhanced using some balancing methods

to equalize the energy inside each cell. It is fundamental to extend the battery capacity in both charging and discharging phases. On the other hand, battery lifetime can be maximized through some current derating strategies used to avoid battery degradation at a low level of SOC. Finally, pack safety is increased by controlling each cell and avoiding any undervoltage, overvoltage, and overcharge faults.

Moreover, the SOC value acts as an input for other calculations such as SOH, cell balancing, and power calculation.

There are basically two main methods used for SOC estimation:

- measuring the battery Open Circuit Voltage, OCV,

- measuring the current provided by the battery.

However, the methods above are very simple and cannot be able to provide accurate results which are required in the automotive field. In recent years, many carmakers have therefore been working to improve the accuracy of SOC estimates using more advanced and robust algorithms.

The goal of this paper is to model a lithium-ion cell by means of an Equivalent Circuit Model ECM and to compare two non-linear Kalman Filter performances in estimating cell SOC.

In section II the battery modelling and the most important SOC estimation algorithms are introduced. In section III the model parameters identification procedure is presented, whereas in section IV the results of the proposed algorithms are discussed and compared.

II. BATTERY MODELLING

A. Battery Cell Model

ECM uses passive electrical components to describe the behaviour of the battery. It has been developed especially for vehicle power management control and BMS. Typically, an ideal voltage source is selected to represent the OCV, additional resistance and capacitance blocks simulate the battery internal resistance and dynamic effects such as the voltage drops due to polarization and mass diffusion phenomena.

There are two categories of ECM: the first uses Electrochemical Impedance Spectroscopy (EIS) to evaluate the cell internal electrical parameters and are called Impedance models. [5], [6]–[8]. The second type of model is the Thevenin model, in particular, the 2nd order Thevenin model has been chosen in this work because it is a trade-off between precision, and lightness [9]. It is made up of an ideal voltage source, a series resistance, a first resistance in parallel with a capacitance and a second resistance in parallel with another capacitance to describe the high non-linear behaviour of the cell. The second RC parallel block can simulate with high fidelity the electrical behaviour of the cell and its voltage response during the transient phase caused by the slow chemical reactions which occur inside the cell. The battery voltage response is evaluated using the next non-linear formula [10]:

$$V(t)=OCV-V_1 e^{-t/\tau_1}-V_2 e^{-t/\tau_2} \qquad (1)$$

However, a coupled electrical and thermal battery models are required to evaluate how both phenomena affect the battery behaviour. At this scope, a previous battery model described and validated in [11] is used. The proposed model (based on the 2nd order Thevenin) solves the energy balance of the cell for the thermal problem according to the equations:

$$\rho c_p \frac{\partial T}{\partial t}=k_r \left(\frac{\partial^2 T}{\partial r^2}+\frac{1}{r}\frac{\partial T}{\partial r}\right)+k_z \left(\frac{\partial^2 T}{\partial z^2}\right)+q \qquad (2)$$

$$q=I(OCV-V)-IT\frac{\partial OCV}{\partial T} \qquad (3)$$

where: ρ, c_p, k_r, k_z are the thermophysical properties of the cell: density, specific heat capacity, thermal conductivity in the radial and axial direction, respectively.

Several SOC estimations have been presented in the literature [12]–[14] and classified in: voltage-based, coulomb counting, direct method, electromotive force, and adaptive technique. The simplest method for SOC estimation is the voltage-based method commonly used for lead-acid battery which are characterized by a quite linear trend of SOC and OCV, thus starting from a voltage measurement is possible to evaluate the battery state of charge through the relationship:

$$OCV(t)=a_1 SOC(t)+a_0 \qquad (4)$$

Where the coefficients a_1 and a_0 are properly tuned to fit the OCV-SOC curve.

The model is very simple, nevertheless, it shows many drawbacks: it does not consider temperature, aging, and C-rate dependencies, it is very sensitive to voltage sensor error especially in the middle range of the voltage curve where it is very flat, thus a small variation of voltage implies high variation of SOC. Moreover, the hysteresis effect is not taken into account, which in turn causes large errors.

Lithium-ion cells are characterized by high non-linear behaviour; thus the voltage-based algorithm becomes unfeasible for this kind of chemistry. Coulomb counting is the most widespread method to calculate the battery state of charge. It consists in the integration of the current over time using the equation:

$$SOC = SOC_0 + \frac{1}{C_n} \int_{t_0}^{t_0+\Delta t} i(t) dt \tag{5}$$

Where: SOC_0 is the state of charge at time zero, C_n is the battery capacity, and i the measured current. Coulomb counting is very simple to be implemented in real-time applications, nevertheless, it has two major drawbacks: first, the impossibility to recover from a wrong SOC_0 initialization, second error accumulation over time due to sensor noise and inaccuracy in current measurement.

To overcome the limits of the Coulomb counting method some model-based adaptive techniques can be used, in which the previous model output is corrected with some measured data to obtain some posterior values and the right state estimation of the system. Kalman filter is one of the most important algorithms for model-based methods.

B. Linear Kalman Filter

The Kalman filter is an effective recursive algorithm able to evaluate the state of a linear dynamic system using some measurements affected by gaussian white noise. To model the system the following linear state-space form is used:

$$\begin{cases} x_k = A_{k-1} x_{k-1} + B_{k-1} u_{k-1} + w_{k-1} \\ y_k = C_k x_k + D_k u_k + v_k \end{cases} \tag{6}$$

Where: x_k is the system state vector at time index k, u_k is the input of the system, y_k is the system output, w_k and v_k are mutually uncorrelated Gaussian white noises, with zero mean and known covariance matrices.

The Kalman filter algorithm is made up of two steps:

1. prediction step, it uses the model equations to predict the states at the present time step;

2. correction step, the algorithm corrects the predicted state using the measured output coming from the real system.

Due to the non-linearity of the battery model, the linear Kalman filter is not suitable to describe the internal state of the system, thus a more advanced non-linear Kalman filter must be used. In this paper, two different algorithms are presented and implemented in the control system:

- Extended Kalman Filter EKF,

- Sigma Point Kalman Filter SPKF

In particular, the full model in state space form $[x_{+1}, y_{k+1}]$ is:

$$\begin{bmatrix} SOC_{k+1} \\ V_{1,k+1} \\ V_{2,k+1} \end{bmatrix} = \begin{bmatrix} 1 & 0 & 0 \\ 0 & 1-\frac{\Delta t}{R_1 C_1} & 0 \\ 0 & 0 & 1-\frac{\Delta t}{R_2 C_2} \end{bmatrix} \begin{bmatrix} SOC_k \\ V_{1,k} \\ V_{2,k} \end{bmatrix} + \begin{bmatrix} \frac{\Delta t}{C_n} \\ \frac{\Delta t}{C_1} \\ \frac{\Delta t}{C_2} \end{bmatrix} i_k \tag{7}$$

$$V_{k+1} = OCV_{k+1} + V_{1,k+1} + V_{2,k+1} - R_{int} i_{k+1} \tag{8}$$

C. Extended Kalman Filter

It is the most widespread application of the Kalman filter when non-linear systems are involved. The algorithm is based on two fundamental assumptions for the estimation of the non-linear function output and covariance. In particular, the expected value of the output state is approximated to the same non-linear function evaluated at the state expected value. Moreover, for covariance estimate, EKF linearizes analytically the model equations through the Taylor series expansion. As for the Linear Kalman Filter, the EKF is made up of two steps, the prediction, and the correction. In the first step the state prediction based on previous states and input is performed, then the covariance prediction and the output guess are calculated according to equations [15]:

$$\hat{x}_k^- \approx f(\hat{x}_{k-1}^+, u_{k-1}, w_{k-1}) \tag{9}$$

$$\Sigma_{\tilde{x},k}^- \approx \hat{A}_{k-1} \Sigma_{\tilde{x},k-1}^- \hat{A}_{k-1}^T + \hat{B}_{k-1} \Sigma_{\tilde{w}}^- \hat{B}_{k-1}^T \tag{10}$$

$$\hat{y}_k^- \approx h(\hat{x}_k^-, u_k, v_k) \tag{11}$$

In the second step, the Kalman gain matrix is calculated using the Taylor series expansion and it is used for the correction of both the state and the covariance of the state:

$$L_k = \Sigma_{\tilde{x},k}^- \hat{C}_k^T \left[\hat{C}_k \Sigma_{\tilde{x},k}^- \hat{C}_k^T + \hat{D}_k \Sigma_{\tilde{v}} \hat{D}_k^T \right]^{-1} \tag{12}$$

$$\hat{x}_k^+ = \hat{x}_k^- + L_k(y_k - \hat{y}_k) \tag{13}$$

$$\Sigma_{\tilde{x},k}^+ = \Sigma_{\tilde{x},k}^- - L_k \Sigma_{\tilde{y},k} L_k^T \tag{14}$$

The proposed model represented in ==**Errore. L'origine riferimento non è stata trovata.**== is made up of the main blocks:

- Blue block, called "GetParams", contains the lookup tables of the electrical circuit parameters both for charging and discharging phases.

- Orange block, contain three different sub-blocks. In the 1st the 2nd order equivalent circuit model is implemented, and it linearizes the non-linear function computing partial derivatives. Moreover, it performs the prediction step to compute the covariance matrices related to the state prediction and the output prediction. The 2nd sub-block evaluates the SOC of the cell through the Coulomb counting algorithm. Finally, a 3rd sub-block calculates the Kalman gain and performs the Kalman filter correction step. It also computes the error between the measured voltage across the cell and the predicted output based on the model, consequently, it applies a correction to the SOC prediction and its covariance matrix.

- Red block thermal problem is solved, in the first moment the heat source is calculated, and it is used in a second moment for the solution of the energy balance through a finite difference to evaluate the thermal field inside the cell.
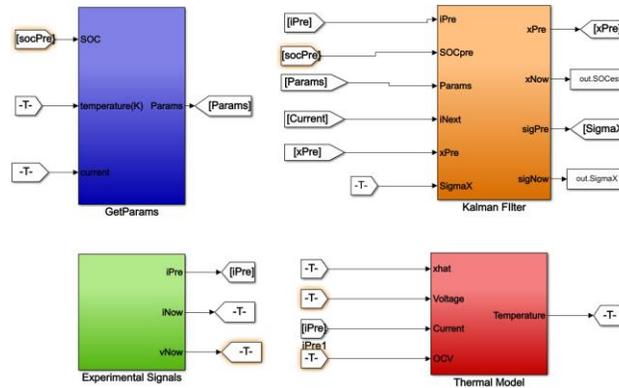

Fig.1. EKF Matlab model

D. Sigma Point Kalman Filter

The EKF is the most common algorithm among non-linear Kalman filters, but it has some drawbacks linked to its assumptions which cause some mistakes in output estimation. To overcome these limits a sigma-points method can be used, where an empirical or statistical linearization is used instead of an analytical linearization. In this way no derivatives must be evaluated, the function can be not differentiable, a better covariance estimation can be calculated with a comparable computational cost.

A suitable number of points X is taken so that their mean and covariance is equal to the mean $\bar{x}$ and covariance $\Sigma_{\tilde{x}}$ of the a priori random variable. The points are the input of the non-linear function which returns them as a set of point Y. The statistics of the transformed point can then be calculated to form an estimate of the non-linearity transformed mean and covariance. Sigma points evaluate a precise number of vectors calculated in a deterministic way. The equations involved in the prediction and correction steps typical of the Kalman filter method are:

$$x_k^- \approx \sum_{i=0}^p \alpha_i^m f(X_{k-1}^{x,+}, u_{k-1}, X_{k-1,i}^{w,+}) \tag{15}$$

$$\Sigma_{\tilde{x},k}^- = \sum_{i=0}^p \alpha_i^c (X_{k,i}^{x,-} - \hat{x}_k^-)(X_{k,i}^{x,-} - \hat{x}_k^-)^T \tag{16}$$

$$\hat{y}_k \approx \sum_{i=0}^p \alpha_i^m h(X_{k,i}^{x,-}, u_k, X_{k-1,i}^{v,+}) \tag{17}$$

$$L_k = \Sigma_{\tilde{x}\tilde{y},k}^- \Sigma_{\tilde{y},k}^- 1 \tag{18}$$

$$\hat{x}_k^+ = \hat{x}_k^- + L_k(y_k - \hat{y}_k) \tag{19}$$

$$\Sigma_{\tilde{x},k}^+ = \Sigma_{\tilde{x},k}^- - L_k \Sigma_{\tilde{y},k} L_k^T \tag{20}$$

III. PARAMETERS IDENTIFICATION

The model parameter identification is based on the current pulse test and has been explained in [16]. The cells under test are LG INR18650−MJ1 3500 mAh. The experimental setup (**Errore. L'origine riferimento non è stata trovata.**) is composed of: The Neware-BTS; 8 LG cells; an environmental chamber; 8 NTC to measure the cell temperatures; a PC for storing and processing data. The Neware-BTS is a programmable electronic load with 16 independent channels. Proprietary software developed in Beond company is used for test programming and for acquiring current and voltage at a sampling frequency of 1Hz. Besides the cell voltage and current, the temperature from each cell is recorded. To set different and constant environmental temperature is used a climatic chamber.
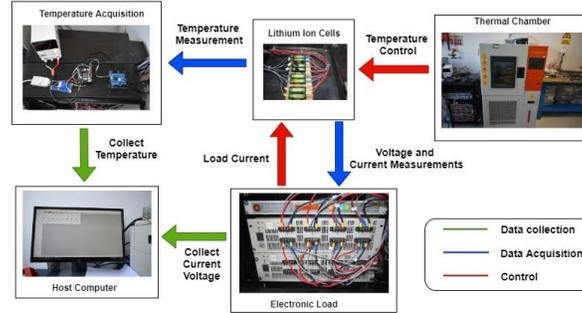

Fig. 2. Experimental setup

The goal of cell characterization is to identify the electrical parameters of the equivalent circuit and its dependencies with respect to SOC, temperature and current. Initially, the cells performed a preconditioning procedure [5]. After preconditioning, a pulse test is performed. The Pulse test is known in different standards also as Hybrid Pulse Power Characterization HPPC test. The cells are excited with constant current pulses, these must always remain within the limits specified by the manufacturers, in terms of voltage, maximum currents and temperatures. The voltage response to these pulses is fitted with a combination of passive elements, resistors, and capacitors, leading to the parametrization of the equivalent circuit model. The voltage relaxation behaviour is provided in Fig. 3.

The OCV is obtained as the last voltage value at the end of the relaxation period, and its accuracy increases with a longer relaxation time. The series resistance R_0 is evaluated as the ratio of the voltage variation V_0 at the end of the current pulse end ΔI:

$$R_0 = V_0/\Delta I \tag{21}$$

The resistance and capacitance in the parallel blocks are calculated by a curve fitting procedure able to provide the non-linear part of the voltage response of the cell $V_1(t)+V_2(t)$, since the double-RC equivalent circuit model response has the form:

$$f = OCV + V_1(1-e^{\frac{\Delta t}{\tau^1}}) + V_2(1-e^{\frac{\Delta t}{\tau^2}}) \tag{22}$$

The fitting process is carried out in MATLAB environment, in particular, lsqnonlin MATLAB function has been used.

HPPC tests have been repeated at the following temperatures: 0°C, 10°C, 20°C, 30°C, and 40°C. Moreover, the C-rate influence has been investigated by repeating the tests at different currents: 1C, 2C, and 3C. This operation was very time consuming but allows to create a model valid for a wide range of operating conditions. This strategy significantly increases the number of estimation steps, but it reduces the number of free parameters in each task increasing the accuracy.
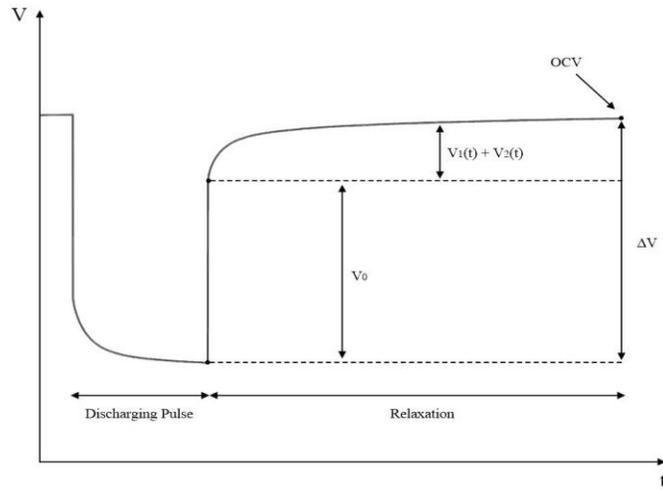
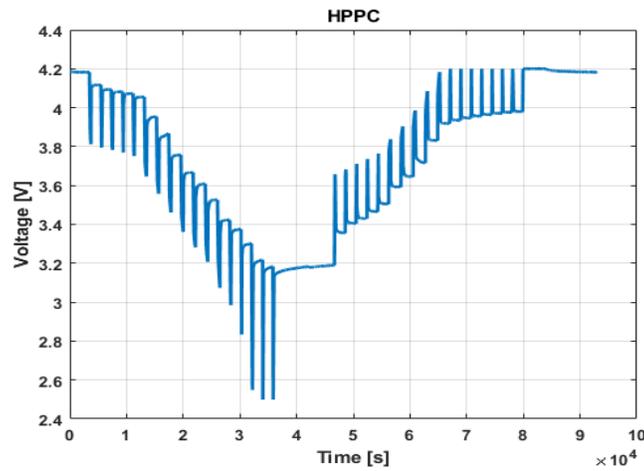Fig. 3. Parameter extraction procedure in discharging phase

Fig. 4. HPPC Voltage Profile

It has been decided to charge and discharge the cells with pulses of different duration. The pulses at high and low SOC were taken while discharging 3% of the cell capacity, while the other pulses discharged 10% of the cell capacity. In this way, it has been collected more data at high and low SOCs, where the cell behaviour is significantly non-linear. After each pulse, the cell observed a rest period of 30 minutes, allowing the cell to reach almost stationarity OCV values (Fig. 4).

IV. RESULTS

In this section, the parameters of the 2nd order Thevenin battery model obtained from the experimental tests are provided. In particular, the dependence of the parameters from SOC, temperature, and current are highlighted. These values are the input for both models Extended Kalman Filter and Sigma Point Kalman Filter. Then, the results obtained from both models are provided and compared in terms of accuracy.

A. ECM Parameters

The extracted parameters are represented in Fig. 5, Fig. 6, and Fig. 7. As mentioned, the parameters are a function of SOC, temperature, and current, nevertheless in the all the figures one variable is kept fixed and the dependence from the other two is evaluated for an effective visualization of the results.

In this paper only the outline of the internal resistance, R_0, is show.
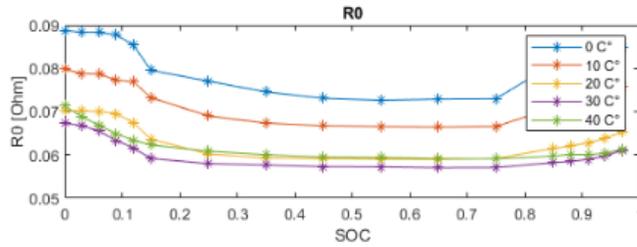
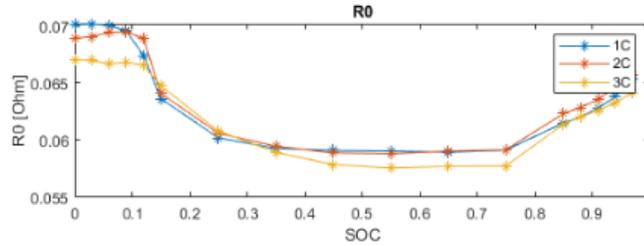Fig. 5.   R0 vs. SOC and Temperature at 1C
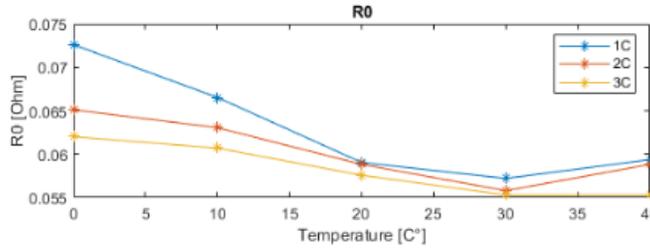

Fig. 6.   R0 vs. SOC and C-rate at 20°C

Fig. 7.   R0 vs. Temperature and C-rate at SOC 55%

B. SOC Estimation Algorithms

A standard driving cycle is selected to validate the proposed models. A current profile is applied to a real cell and its voltage response is compared with the output of both models to evaluate the best SOC estimation strategies. Different performance indices were used: root mean square error, absolute mean error and SOC variance. Different scenarios were taken into account, in the first one the current profile typical of a WLTP Class 3 driving cycle is used and the SOC initial value is set correctly to its maximum values (Fig. 8, Fig. 9, Fig. 10 and Fig. 11).
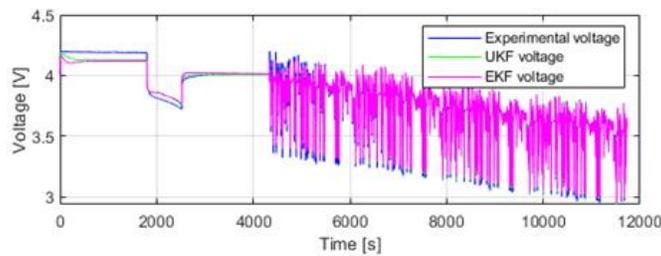

Fig. 8.   WLTP Test 1 vs. Models: Voltage Comparison
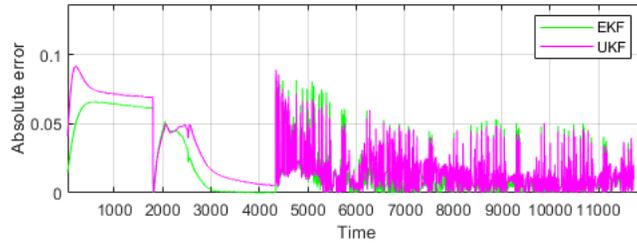
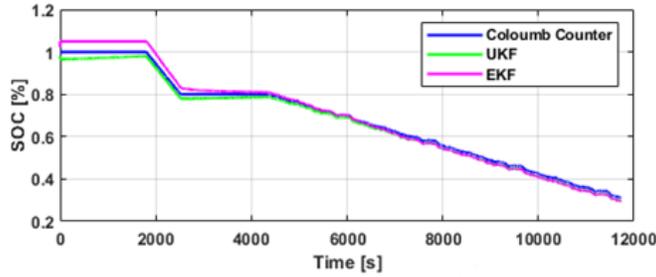Fig. 9.   WLTP Test 1 vs. Models: Voltage absolute error
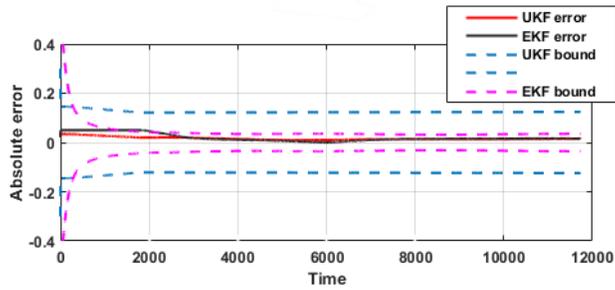

Fig. 10.   WLTP Test 1 vs. Models: SOC Comparison

Fig. 11.   WLTP Test 1 vs. Models: SOC absolute error

TABLE I. MODELS RESULTS FOR WLTP TEST 1

Algorithm	Performance Index		
	SOC RMSE [%]	V RMSE [mV]	SOC Variance
EKF	0.024	33.7	1.77 e-4
UKF	0.0025	33.3	0.001

As it is possible to see from the table above, both filters perform very well minimizing the value of the state of charge root mean square error. The UKF is more accurate than EKF, nevertheless it shows a higher variance.
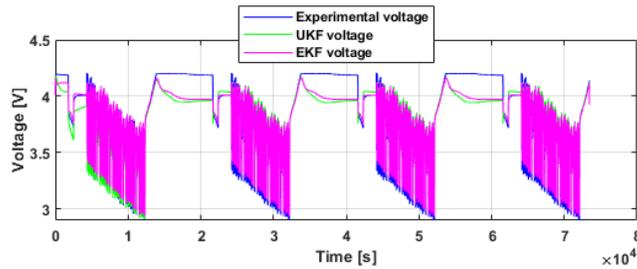

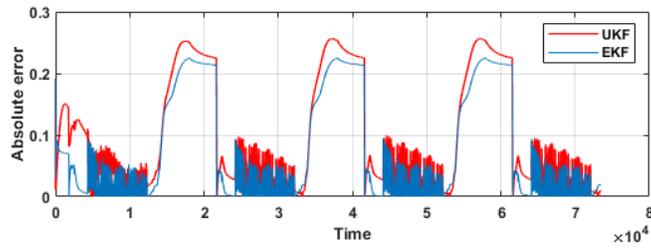Fig. 12.   WLTP Test 2 vs. Models: Voltage Comparison

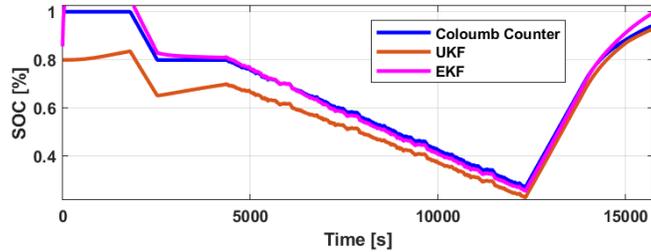Fig. 13.   WLTP Test 2 vs. Models: Voltage absolute error

Fig. 14.   WLTP Test 1 vs. Models: SOC Comparison

In the second scenario, the cell is subjected to 4 WLTP driving cycles and a wrong SOC initialization is made to evaluate the ability of both the strategies to converge to correct SOC values (Fig. 12, Fig. 13 and Fig. 14).

Although both algorithms cannot effectively simulate the battery voltage response during the rest periods, they converge to the real voltage as soon as the battery contactors are closed. In particular, the performance indices of the table below show how the EKF has a faster convergence to the correct SOC, a lower SOC RMSE and a lower mean SOC variance with respect to the UKF.

TABLE II. MODELS RESULTS FOR WLTP TEST 2

Algorithm	Performance Index		
	SOC RMSE [%]	V RMSE [mV]	SOC Variance
EKF	0.032	116	2.86 e-4
UKF	0.048	116	0.0017

V.   CONCLUSIONS

In this paper, two SOC estimation algorithms for lithium-ion battery were developed and validated through experimental test properly made. The battery behaviour is simulated through a 2nd order Thevenin equivalent circuit model which works accurately and requires low computational cost even when highly dynamic current profiles are involved. The ECM parameters (SOC, temperature and current dependent) have been evaluated by means of several hybrid pulse power characterization tests performed at different temperatures and C-rates. Also, the battery thermal response is evaluated to predict the cell temperature evolution and to capture the strict link between electrical and thermal phenomena occurring inside the cell.

The model was validated by means of a highly dynamic current profile providing a good precision in voltage response evaluation with a root mean square equal to 0.75% of the nominal cell voltage. Different scenarios were used to evaluate the performances of the proposed SOC algorithms. In the first case, a correct SOC initialization is set, the SOC estimation precision of the UKF algorithm was significantly higher than the EKF. In the second scenario, SOC was initialized to a wrong value to evaluate the speed of the convergence. The EKF showed a faster speed convergence with respect to UKF. Moreover, the EKF performed better also in terms of SOC variance which was significantly smaller than the value obtained from the UKF algorithm.

REFERENCES

[1]   M. Ehsani, *Modern electric, hybrid electric, and fuel cell vehicles*, Third edition. Boca Raton: Taylor & Francis, CRC Press, 2018.
[2]   M. Casisi, P. Pinamonti, e M. Reini, «Increasing the Energy Efficiency of an Internal Combustion Engine for Ship Propulsion with Bottom ORCs», *Appl. Sci.*, vol. 10, n. 19, pag. 6919, ott. 2020, doi: 10.3390/app10196919.
[3]   R. Luque, A c. di, *Handbook of biofuels production: processes and technologies*, Second edition. Amsterdam Boston Cambridge Heidelberg London New York Oxford Paris San Diego San Francisco Singapore Sydney Tokyo: Woodhead Publishing, 2016.

[4]   O. Egbue e S. Long, «Barriers to widespread adoption of electric vehicles: An analysis of consumer attitudes and perceptions», *Energy Policy*, vol. 48, pagg. 717–729, set. 2012, doi: 10.1016/j.enpol.2012.06.009.

[5]   F. Saidani, F. X. Hutter, R.-G. Scurtu, W. Braunwarth, e J. N. Burghartz, «Lithium-ion battery models: a comparative study and a model-based powerline communication», *Adv. Radio Sci.*, vol. 15, pagg. 83–91, set. 2017, doi: 10.5194/ars-15-83-2017.

[6]   S. Scavuzzo *et al.*, «Simplified Modeling and Characterization of the Internal Impedance of Lithium-Ion Batteries for Automotive Applications», in *2019 AEIT International Conference of Electrical and Electronic Technologies for Automotive (AEIT AUTOMOTIVE)*, Torino, Italy, lug. 2019, pagg. 1–6. doi: 10.23919/EETA.2019.8804553.

[7]   E. Locorotondc *et al.*, «Modeling and simulation of Constant Phase Element for battery Electrochemical Impedance Spectroscopy», set. 2019 Consultato: dic. 15, 2019. [In linea]. Available at: https://ieeexplore.ieee.org/document/8895597/

[8]   E. Locorotondo *et al.*, «Electrochemical Impedance Spectroscopy of Li-Ion battery on-board the Electric Vehicles based on Fast nonparametric identification method», in *2019 IEEE International Conference on Environment and Electrical Engineering and 2019 IEEE Industrial and Commercial Power Systems Europe (EEEIC / I&CPS Europe)*, Genova, Italy, giu. 2019, pagg. 1–6. doi: 10.1109/EEEIC.2019.8783625.

[9]   D. Cittanti, A. Ferraris, A. Airale, S. Fiorot, S. Scavuzzo, e M. Carello, «Modeling Li-ion batteries for automotive application: A trade-off between accuracy and complexity», giu. 2017, pagg. 1–8. doi: 10.23919/EETA.2017.7993213.

[10]   A. Rizzello, S. Scavuzzo, A. Ferraris, A. G. Airale, e M. Carello, «Dynamic Electro-Thermal Li-ion Battery Model for Control Algorithms», in *2020 AEIT International Annual Conference (AEIT)*, set. 2020, pagg. 1–6. doi: 10.23919/AEIT50178.2020.9241107.

[11]   A. Rizzello, S. Scavuzzo, A. Ferraris, A. G. Airale, e M. Carello, «Electrothermal Battery Pack Model for Automotive Application: Design and Validation», in *2020 AEIT International Conference of Electrical and Electronic Technologies for Automotive (AEIT AUTOMOTIVE)*, nov. 2020, pagg. 1–6. doi: 10.23919/AEITAUTOMOTIVE50086.2020.9307377.

[12]   S. Piller, M. Perrin, e A. Jossen, «Methods for state-of-charge determination and their applications», *J. Power Sources*, vol. 96, n. 1, pagg. 113–120, giu. 2001, doi: 10.1016/S0378-7753(01)00560-2.

[13]   K. W. E. Cheng, B. P. Divakar, H. Wu, K. Ding, e H. F. Ho, «Battery-Management System (BMS) and SOC Development for Electrical Vehicles», *IEEE Trans. Veh. Technol.*, vol. 60, n. 1, pagg. 76–88, gen. 2011, doi: 10.1109/TVT.2010.2089647.

[14]   W. Waag e D. U. Sauer, «Adaptive estimation of the electromotive force of the lithium-ion battery after current interruption for an accurate state-of-charge and capacity determination», *Appl. Energy*, vol. 111, pagg. 416–427, nov. 2013, doi: 10.1016/j.apenergy.2013.05.001.

[15]   G. L. Plett, *Battery management systems. Volume 2: Equivalent-circuit methods / Gregory L. Plett*. Boston London: Artech House, 2016.

[16]   A. Rizzello, S. Scavuzzo, A. Ferraris, A. G. Airale, e M. Carello, «Temperature-Dependent Thévenin Model of a Li-Ion Battery for Automotive Management and Control», in *2020 IEEE International Conference on Environment and Electrical Engineering and 2020 IEEE Industrial and Commercial Power Systems Europe (EEEIC / I&CPS Europe)*, Madrid, Spain, giu. 2020, pagg. 1–6. doi: 10.1109/EEEIC/ICPSEurope49358.2020.9160544.